Ionization in coplanar symmetric $(e,2e)$ experiments of N$_2$ and CO at intermediate energies

S. Rioual, G. Nguyen Vien, and A. Pochat

Laboratoire des Collisions Electroniques et Atomiques, UFR Sciences et Techniques, 6 avenue V. Le Gorgeu, Boîte Postale 809, 29285 Brest Cedex, France

(Received 23 October 1995; revised manuscript received 29 July 1996)

Measurements of the triple differential cross sections in coplanar symmetric energy sharing geometry for the two isoelectronic molecules N$_2$ and CO are presented between 90 and 400 eV incident energy. At 400 eV, our results are compared to those of previous $(e,2e)$ experiments done in other geometries and to photoionization data. At this incident energy, a comparison is also made with the plane wave impulse approximation (PWIA). Our calculations show that this does not perfectly describe the measured cross sections. Measurements made over an extended angular range, 30°–120°, present two maxima: that at large angle results from backscattering of the projectile prior to ionization of the target and is not explained by the PWIA. As energy is decreased, as for atoms, the relative importance of the low angle peak diminishes and that of the large angle peak increases: we then lack an adequate theoretical model and only comparison with data obtained for atomic targets under similar kinematical conditions is possible. Our high energy resolution permits the observation of several satellite structures for both target molecules, in particular for CO. At 400 eV, the assignment of these to different residual ion primary hole states correlates with the forms of the angular distributions. [S1050-2947(96)02612-1]

PACS number(s): 34.80.Gs

I. INTRODUCTION

In $(e,2e)$ experiments, a scattered and an ejected electron are detected in coincidence following electron impact ionization of the target. This has been found to provide the most suitable tool, on the one hand to study the dynamics of ionization by electron impact [1], on the other to investigate the electronic structure of atoms and molecules [2,3]. At low and intermediate incident energies, the triple differential cross sections (TDCS) are found to be highly sensitive to "multiple collision" type dynamical effects. These are essentially of two sorts: antecollision backscattering (ACB) of the projectile prior to the ionization of the target and postcollision interaction (PCI) between the two outgoing electrons. They become particularly evident under the coplanar symmetric energy sharing geometry. Following on the early work of Pochat et al. [4] and that of Frost, Freienstein, and Wagner [5], many experiments have been made in this geometry to look for such effects in light atomic targets [6–8]. These cover a range of incident energies from near threshold up to 500 eV. Measurements in excess of twice threshold show a forward peak near 45°, due to a binary collision between the two colliding electrons, and a backward peak at angles of the order of 120°, explained by a mainly elastic ACB process [4]. In measurements on rare gas targets at intermediate energies (neon [6,9], xenon [10], and argon [11]), the presence of a proportionately more important large angle peak indicates the existence of a backscattering process stronger than that in ionization of hydrogen and helium. On the theoretical side, so long as the incident energy remains larger than about 100 eV the distorted wave Born approximation (DWBA) calculations of Whelan et al. [12], including elastic ACB effects but uncorrected for postcollision interaction, give quite good agreement with the data. At lower energy the backward peak becomes as large as the forward one and, as threshold is approached, the two merge to form a single "Wannier" peak

near 180° relative angle (90° symmetric angle) [7,8]. To extend calculations down towards threshold, the inclusion together of PCI, ACB, and target polarization is necessary in order to describe the ionization process correctly [13–15].

The few investigations of ionization dynamics for molecular targets that have been made are in asymmetric coplanar geometry at intermediate energies on H$_2$ [16] and N$_2$ [16,17]. Experiments on C$_2$H$_2$ [18] and H$_2$ [19] also exist at higher energies. The early experiments on a N$_2$ target by Jung et al. [16] at 100 eV and the later ones by Avaldi et al. [17] at 300 eV both took an energy for the scattered electron very much larger than that of the ejected electron. Under such conditions the relative magnitude of the recoil lobe depends strongly on the incident energy. Jung et al. [16] found this lobe to be often insignificant, but the experiments of Avaldi et al. [17] show a stronger backscattering process than for atomic hydrogen and helium.

The only theoretical model in current use to describe ionization of molecular targets is the plane wave impulse approximation (PWIA), extensively exploited by McCarthy and Weigold [2]. The validity of this approximation from 400 eV to high incident energy in noncoplanar symmetric geometry has been demonstrated for N$_2$ target molecules by Weigold et al. [20] and for CO molecules by Dey et al. [21]. The model also reproduces measurements on N$_2$ of Avaldi et al. [22] made in an asymmetric coplanar arrangement with ionization kinematics which follow the Bethe ridge. However, it requires the computation of the half-off-shell Coulomb T matrix. According to the way in which singularities are treated in this matrix, three different prescriptions are available for this (McCarthy and Roberts [23]). In the "standard" [24] formulation for evaluation of the general Coulomb T matrix there is complete discontinuity between on- and off-shell cases. The Ford method [25] for the half-off-shell T matrix, preferred by McCarthy, Weigold, and collaborators, gets rid of on-shell discontinuities only. The

''regularized'' [26] one eliminates all discontinuities. In the coplanar symmetric geometry employed here, at high enough energy and for angles in the region of 45° (forward scattering), the collision is expected to be of a binary nature. The PWIA should then be valid, except for the problem of how to calculate the half-off-shell Coulomb T matrix. At the high energies used for spectroscopic purposes, all prescriptions converge to the same result and there is no problem. But at 400 eV they give different shapes, so we find it interesting to look at the validity of the PWIA in this respect.

Electron impact ionization of molecules is a more complex (and interesting) problem than ionization of atoms because of the presence of multiple attractive nuclear potentials and, in the case of any linear molecule, because of cylindrical symmetry around the internuclear axis. A full calculation of DWBA type requires the use of products of three rotation operator matrix elements to go from the molecular to the laboratory frame, and integration over molecular orientations does not greatly simplify the formulation. In this paper, ACB effects for N_2 and CO targets are investigated experimentally between 90 and 400 eV over a wide angular region but our results can only be compared with previous measurements on atoms for the moment. In the low energy region, we expect dynamical ACB and also PCI effects as observed for atomic targets.

Our energy resolution is adequate for us to be able to observe clearly separated satellite structures, noted in the pioneer $(e,2e)$ measurements in noncoplanar symmetric geometries [20,21] but too weak to be resolved, and corresponding to structures seen in photoelectron spectroscopy (PES). The origin of these structures, both in $(e,2e)$ and in PES experiments, has been discussed by Amusia and Kheifets [27]. They are due mainly to correlation effects in the target or in the residual ion final state (shake-up and shake-off type effects). Recently, a more accurate study of N_2 was performed by Cook *et al.* [28] with improved energy resolution but the structures were still not clearly separated. Contrarily to these previous $(e,2e)$ experiments, the TDCS measured in our geometry depend not only on the momentum density of the target orbital which is ionized, but also on the kinematical factor which varies strongly with polar angle. It is not possible for us, even at 400 eV, to separate completely the effects of the collision kinematics and of the electronic structure, but the differences observed between the experimental TDCS of each ion state do manifest the effects of correlation.

The present $(e,2e)$ experiments are unconventional for ionization of molecules in that a low to intermediate energy region and a wide angular range are covered. Our motivation for such measurements of the TDCS for simple molecules in the gas phase is not only, as mentioned above, to study the ionization dynamics and to provide test data for a DWBA type theoretical model which is being developed. We also wish to catalog low and intermediate energy TDCS for use in the analysis of future $(e,2e)$ experiments on ionization of atoms and molecules adsorbed on surfaces [29]. The paper is organized as follows. In Sec. II the experiment is briefly described. Section III summarizes the theoretical PWIA treatment. Sections IV and V discuss the results obtained on the N_2 and CO molecules, respectively.

II. EXPERIMENT

In the coplanar symmetric energy sharing geometry, the two outgoing electrons have the same energy and the plane containing their momenta $\mathbf{k}_a$ and $\mathbf{k}_b$ also contains the momentum $\mathbf{k}_0$ of the incident electron. Their directions make identical polar angles $\theta = \theta_a = \theta_b$ with its direction. The apparatus has been described elsewhere by Pochat *et al.* [30] and was recently used to study TDCS for neon [9]. The residual gas pressure in the chamber is around 5×10^{-6} torr. The energies and angles of the two electrons emerging from the collision center are determined using two identical 127° electrostatic analyzers; detection is made by channeltrons. The angular resolution of the analyzers is about ±1°. At 45° and 400 eV, the average coincidence rate is of the order of 10 counts/sec for ionization from the outermost orbitals and decreases to about 10^{-3} counts/sec for weaker structures. The coincidence energy resolution used in the investigation of the three first states of N_2^+ is about 0.74 eV, corresponding to an overall resolution of 1 eV. This enables us to resolve the two first states of the ion, separated by only 1.4 eV. For the first two states of the CO^+ ion, separated by 2.9 eV, and for the inner hole ion state of both molecules, the overall energy resolution used is 1.2 eV.

Binding energy spectra were obtained by varying the incident electron energy while keeping fixed the angles θ as well as the energies of the two detected electrons. The angular distributions of the TDCS of the different ion states have been measured at an incident energy of $E_0 + \epsilon$: E_0 is the energy used for detachment of an electron from the outermost orbital, leaving the residual ion in its ground state. ϵ is the energy of the excited ion state with respect to the ground state. In our present work, the cross sections are not given on an absolute scale. However, since the detection efficiencies of the analyzer systems, the target beam flux, and the electron beam current and intensity profile remain unchanged over the whole energy range studied for a given E_0, the relative intensity of the different ion states is obtained directly. For the different targets, at each energy, experimental data are normalized to unity for ionization from the outermost orbital at 45°.

III. THEORETICAL CONSIDERATIONS

Within the framework of the Born-Oppenheimer approximation and applying rotational and vibrational closure to the final unresolved rotational and vibrational states, the PWIA differential cross section for the electron impact ionization of a molecular target is given by McCarthy and Weigold [2] as

$$\frac{d^5\sigma}{d\hat{k}_a d\hat{k}_b dE} = (2\pi)^4 \frac{k_a k_b}{k_0} f_{ee} (4\pi)^{-1} \int d\hat{q}\, G_f(\mathbf{q}), \quad (1)$$

where $\mathbf{q}$ is the momentum of the struck electron in the target system, G_f is the structure factor for an interaction leading to a residual molecular ion in state f, and

$$f_{ee} = |\langle \mathbf{k} | T_{ee}(k^2) | \mathbf{k}' \rangle|^2, \quad (2)$$

where $\langle \mathbf{k} | T_{ee}(k^2) | \mathbf{k}' \rangle$ is the half-off-shell Coulomb T matrix with

$$\mathbf{k}=\tfrac{1}{2}(\mathbf{k}_a-\mathbf{k}_b), \quad \mathbf{k}'=\tfrac{1}{2}(\mathbf{k}_0+\mathbf{q}). \tag{3}$$

This has the same form as the analogous expression for the case of an atomic target. For energy sharing in a symmetric geometry, following McCarthy and Roberts [23], the modulus square of this Coulomb T matrix is given by

$$|\langle\mathbf{k}|T_{ee}(k^2)|\mathbf{k}'\rangle|^2=N^\gamma|T_{ee}^{\mathrm{Ruth}}|^2, \tag{4}$$

where T_{ee}^{Ruth} is the half-on-shell Rutherford scattering amplitude and

$$N=\frac{2\pi\eta}{[\exp(2\pi\eta)-1]}, \tag{5}$$

with $\eta=1/2k$.

Regularized [26], Ford [25], and "standard" [24] forms of the half-off-shell Coulomb T matrix elements are obtained by setting $\gamma=0$, 1, and 2, respectively.

For closed shell molecular targets it is customary to make the target Hartree-Fock approximation (THFA). In this case, G_f becomes

$$G_f(\mathbf{q})=(2j+1)S_{j\alpha}^f|\phi_{j\alpha}(\mathbf{q})|^2, \tag{6}$$

where the spectroscopic factor $S_{j\alpha}$ is the probability of finding the single-hole configuration $(\phi_{j\alpha})^{-1}$ in the ionic state f and $(2j+1)$ is the multiplicity of the initial state molecular orbital $\phi_{j\alpha}(\mathbf{q})$.

We note that in Weigold's out of plane experiments it is necessary to consider a fivefold differential cross section, but it is convenient to revert to the habitual terminology of threefold differential cross sections in the coplanar symmetric case considered here.

The spherically averaged PWIA-THFA structure factor was evaluated in detail by McCarthy and Weigold [2]. For N_2 and CO, the spherically averaged momentum distribution for each outer valence electron transition has been computed using the self-consistent-field (SCF) double-ζ basis molecular wave functions of Snyder and Basch [31]. Because their implementation is straightforward the latter are commonly used for theoretical comparison in electron momentum spectroscopy of molecules, for instance by Cook *et al.* [28] for N_2 and by Dey *et al.* [21] for CO. The spectroscopic factors used in our calculations are also those computed by these authors. Cross sections are then obtained by evaluating f_{ee} for regularized, Ford, and standard forms of the half-off-shell Coulomb T matrix. We decided to compare our measurements to the impulse approximation at a fixed incident energy of 400 eV irrespective to the target. At lower energy, our experience in low energy impact ionization is that the physical phenomena (notably backscattering effects) are sensitive to the ratio of impact energy to ionization potential rather than to impact energy itself. So we use incident energies for both molecules in approximately the ratio 14.1:15.6.

IV. THE N$_2$ MOLECULE

A. Binding energy spectra

Figure 1(a) presents the binding energy spectrum in the region 12–28 eV obtained at $\theta=50°$, $E_0=400$ eV, and with an overall energy resolution of 1 eV. On this spectrum, the
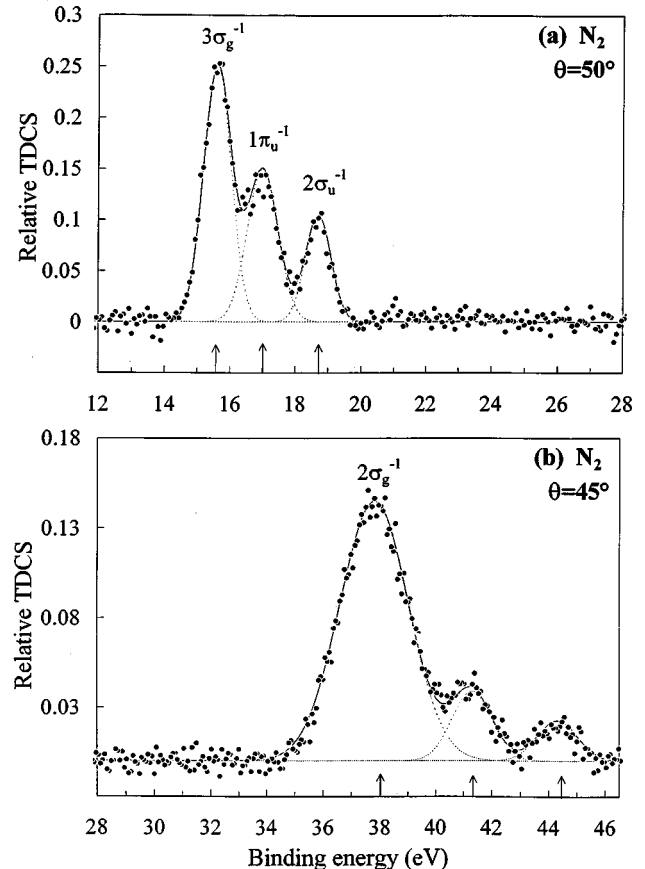

FIG. 1. Binding energy spectra of N_2 at 400 eV incident energy. (a) and (b) have been carried out, respectively, with the overall energy resolutions of 1 and 1.2 eV. In (a), the three peaks correspond to ionization of an electron from a particular molecular orbital. In (b), the broad peak is dominated by ionization from the $2\sigma_g$ orbital. The arrows indicate the positions of the observed ion states. Data are normalized to unity for ionization from the outermost orbital at 45°.

three peaks which correspond to the removal of an electron from the $3\sigma_g$, $1\pi_u$, and $2\sigma_u$ target orbitals are clearly separated. The data are fitted, by means of a χ^2 curve fitting program, using Gaussian functions centered on the energies corresponding to the $(3\sigma_g)^{-1}$, $(1\pi_u)^{-1}$, and $(2\sigma_u)^{-1}$ residual ionic states. A slightly broader one is chosen to represent the $(1\pi_u)^{-1}$ state than for the others since its width is known to be large. The spectrum in Fig. 1(a) was taken at 50° to improve the visibility of the different structures. On the other hand, the 28–46 eV binding energy spectrum presented in Fig. 1(b) was taken at 45°, leading to a maximum for the amplitude of the structures; an overall energy resolution of 1.2 eV is also chosen to improve the coincidence rate. The main peak at 38 eV is extremely broad and is identified to be ionization of the $2\sigma_g$ orbital. Two additional weak structures are observed at about 41.3 and 44.4 eV. This spectrum is similar to that obtained by Cook *et al.* [28] at 500 eV, $\theta=45°$, and with an out of plane azimuthal angle $\phi=0.3°$. The peak at 38 eV is found to have the same width of about 3 eV full width at half maximum (FWHM) and also the same intensity. In contrast to this previous work where only a shoulder appears on the high energy side of the main peak, the structures observed here are well separated.
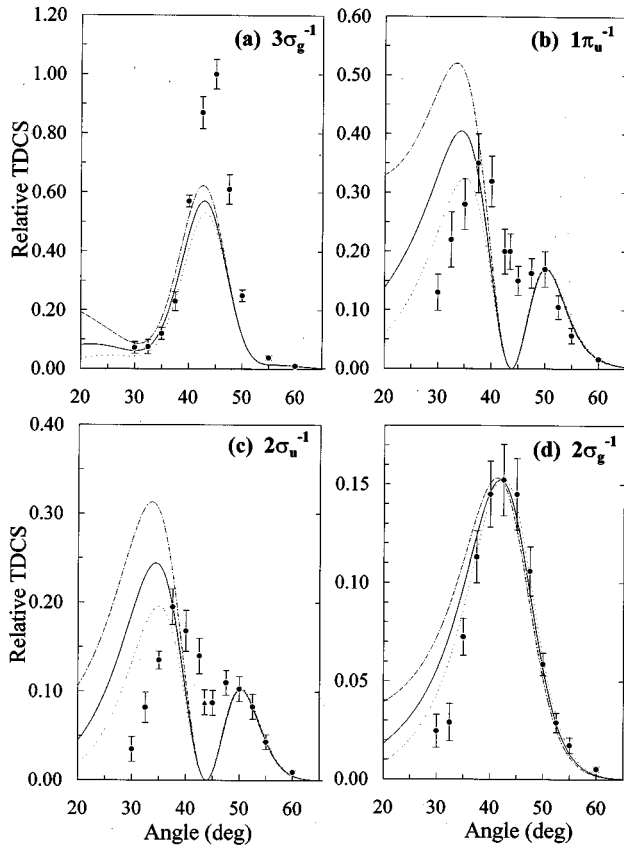
FIG. 2. 400 eV coplanar symmetric TDCS for ionization from the $3\sigma_g$ (a), $1\pi_u$ (b), $2\sigma_u$ (c), and $2\sigma_g$ (d) orbitals of N_2. PWIA calculations for the Ford (—), regularized (– – –), and standard (···) forms of the half-off-shell Coulomb T matrix. Theoretical calculations are normalized to the data for ionization from the $2\sigma_u$ orbital at 50° except in (d) where they are normalized to the data at 42.5°.

B. Angular distributions

At $E_0=400$ eV, the angular distributions of the TDCS between 30° and 60° performed for the ion states due to one electron transitions are presented in Fig. 2. The TDCS for ionization from the $3\sigma_g$ and $2\sigma_g$ orbitals in Figs. 2(a) and 2(d) both have a maximum near 45°, which corresponds to a momentum of the target electron almost equal to zero. However, it is noticeable that the angular widths of these TDCS are quite different. The shapes of the TDCS for ionization from the $1\pi_u$ and $2\sigma_u$ orbitals in Figs. 2(b) and 2(c) present two maxima, coming from binary collisions corresponding to a particular momentum value of the target electron which is knocked out. For the first maximum at small angles, the target and colliding electron have their momentum in the same direction; these latter are in opposite direction for the second maximum near 50°. The first peak is always considerably larger than the second one and the only significant difference between the TDCS for these two orbitals is their relative intensity. An equivalent shape was found by Fuss *et al.* [32] in coplanar symmetric geometry for ionization of p electrons of atoms. In both previous $(e,2e)$ studies [20,28] using a noncoplanar symmetric geometry a deep minimum (theoretical zero) was found between the two peaks, but in our symmetric coplanar geometry we observe only a relatively shallow minimum.

Cook *et al.* [28] emphasize the fact that the quality of the basis set for the SCF calculations is essential to describe accurately the momentum distributions of N_2 so as to get agreement with this noncoplanar geometry experiment. SCF wave functions, expanded on a basis set of triple-ζ functions improved by inclusion of polarization functions, give better results than the less elaborate Snyder and Basch wave functions [31]. Although the latter provide a fairly correct description of the $1\pi_u$, $2\sigma_u$, and $2\sigma_g$ orbitals they do not do so for the $3\sigma_g$ one. Thus the normalization of our (relative) measurements to our calculations using these wave functions was made for ionization from the $2\sigma_u$ orbital, on the second maximum. At 400 eV and for the high angles, the calculations give correct agreement in shape and magnitude with the data for ionization from the $1\pi_u$ and $2\sigma_u$ orbitals. This is not the case for the low angles where the calculations, whatever the prescription used to get the half-off-shell Coulomb T matrix, systematically overestimate the cross sections and shift all the maxima towards small angles. For ionization from the $3\sigma_g$ orbital, our calculations underestimate the magnitude of maximum. Similar disagreement is found in the work of Cook *et al.* [28] at low momentum $|\mathbf{q}|$ of the target electron. This discrepancy is partly explained by the inadequacy of the wave functions used to describe this orbital. At 400 eV, Weigold *et al.* [20] showed that PWIA calculations are not fully able to describe ionization from the $2\sigma_g$ orbital. Even at this energy, wave function distortions appear to be significant for ionization of this inner orbital and have the effect of reducing the magnitude of the TDCS relative to that for ionization of less tightly bound orbitals. However, the shape of the TDCS, which remains practically unchanged from 400 to 1200 eV, is correctly reproduced by PWIA calculations. Thus, in Fig. 2(d), we make only a comparison between our data and the shape of the TDCS given by the PWIA calculation. As for ionization from the three outermost orbitals, shown in Figs. 2(a)–2(c), disagreement is found at small angles.

In noncoplanar symmetric geometry, except for the $(2\sigma_g)^{-1}$ residual ion state, the PWIA calculations describe correctly the ionization process at incident energy as low as 400 eV. It is also found to be satisfactory in the experiments made by Avaldi *et al.* [22] at 1500 eV incident energy, in coplanar asymmetric geometry with 100 eV ejected electron. Since use of a plane wave would thus appear to be adequate to describe outgoing electrons with about 200 eV energy under both these types of kinematical condition, the discrepancy between our calculations and experiments at low angles for 400 eV is most probably the consequence of our combination of coplanar symmetric geometry and energy sharing. This causes $\mathbf{k}_0$, $\mathbf{q}$, and $\mathbf{k}'$ to be in the same direction, whereas $\mathbf{k}$ is perpendicular to them [see Eqs. (2) and (3)]. Any change, even small, in the direction of $\mathbf{k}_0$, such as would be caused by antecollision elastic scattering of the projectile, disturbs this rather particular condition and so could have disproportionate large effect. It is probably this that fills in the deep minimum predicted by the PWIA approximation, which describes the binary collision of the projectile by the electron which is ejected but does not take account of its scattering by the target as a whole. The absence of the very deep minimum in coplanar symmetric geometry has already been noted by the work of Fuss *et al.*
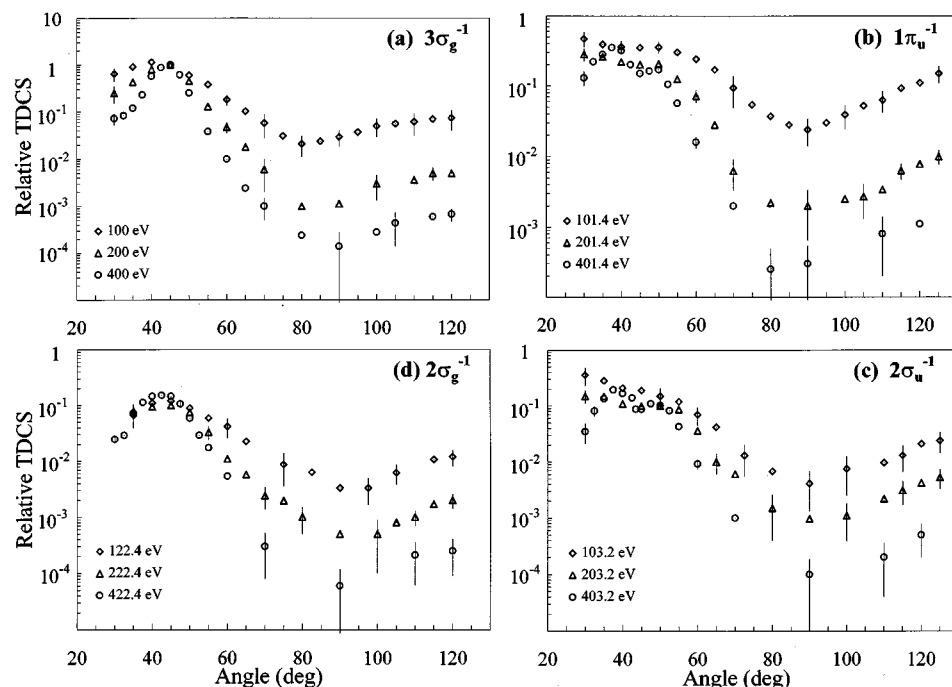
FIG. 3. Coplanar symmetric TDCS for ionization from the $3\sigma_g$ (a), $1\pi_u$ (b), $2\sigma_u$ (c), and $2\sigma_g$ (d) orbitals of N_2. The energy E_0 is 100 eV ($\diamond$), 200 eV ($\triangle$), and 400 eV ($\bigcirc$). Normalization as in Fig. 1.

[32] using a better angular resolution and made at higher incident energy, where the PWIA is expected to be well founded. To explain this discrepancy it is not sufficient to consider the angular resolution as such but one also should rather evaluate its effect on the uncertainty in the momentum $\mathbf{q}$ around $|\mathbf{q}|=0$. Several methods for incorporating the momentum resolution in calculations have been proposed. The study of Duffy et al. [33] demonstrates the importance of such effects in the TDCS for the noncoplanar symmetric geometry. They should be even more important in our geometry than in noncoplanar symmetric or coplanar asymmetric geometries and could also help to explain why no very deep minimum is observed. Additional experiments which we have made at 500 eV give a slightly better agreement between calculations and measurements than that found at 400 eV, particularly at low angles. But although the minimum becomes a bit deeper at this higher energy, it never goes as low as the value predicted by the PWIA calculations.

Experiments have also been performed over a large angular region and at lower energy, to study antecollision backscattering effects. The TDCS for ionization of an electron from the $3\sigma_g$ orbital at 100 and 200 eV incident energy are compared in Fig. 3(a) with that for 400 eV. The data show a behavior very similar to that previously observed in electron impact ionization of a helium $1s$ orbital. Two peaks are observed: the first, near 45°, is explained by a binary collision between the projectile and the ejected electron; the second, at large angles, by an ACB process. When the energy decreases, we observe a stronger backscattering effect together with a shift of the deep minimum from the vicinity of 90° toward lower angle; the first peak at about 45° is also shifted in the same manner. We note that the relative intensity of the backward peak is stronger in the case of a N_2 target than for helium; this could be because of the more important attractive field created by the two nuclei of the molecule. In Figs. 3(b) and 3(c), data are given for the $(1\pi_u)^{-1}$ and for the $(2\sigma_u)^{-1}$ residual ionic states. At 400 eV the ionization pro-

cess is dominated by the binary collision and the small value of the cross section at large angle leads to data exhibiting large error bars. With decreasing the energy, the minimum located near 45° becomes less pronounced and the first maximum is shifted towards low angles; the same observation is valid for ionization of the p shell of atoms. Contrary to the case of the $3\sigma_g$ orbital, the minimum at about 90° seems not to shift towards low angles. A backward peak, increasing in magnitude as the incident energy decreases, is also observed: we note that the ACB affects are more important than for the $(3\sigma_g)^{-1}$ ionic state. This again resembles the situation for atomic targets, where TDCS for ionization from asymmetric orbitals show more important ACB effects than does ionization of the $1s$ shell of helium. The importance of this second order process is comparable to that observed on Ne($2p$) [6,9] or Ar($3p$) [11] in an energy region similar relative to the binding energies of the orbitals. At 100 eV, it seems that this effect becomes more important for the $(1\pi_u)^{-1}$ state than for all the other states. We also find a less pronounced minimum near 90°. At low angles, we note that the shape of the cross section for the two asymmetric orbitals tends to be different at the lowest energy; a flattening appears for the $(1\pi_u)^{-1}$ ionic state which is not present in the $(2\sigma_u)^{-1}$ one. This difference could be induced by the π and σ characters of the orbital from which the electron is ejected. Data for the $(2\sigma_g)^{-1}$ ionic state are presented in Fig. 3(d). The general behavior is similar to that observed for the $(3\sigma_g)^{-1}$ ionic state, but the minimum of the TDCS is located at larger angles. A similar behavior is observed for ionization of the $2s$ inner shell of Ne [9]. In addition, we note that the backward peak is more important for the innermost than for the outermost $3\sigma_g$ orbital. This larger backscattering process could be explained by the location of the $2\sigma_g$ orbital in a region where the nuclear attraction is stronger; however, it remains lower than for the two asymmetric orbitals.

In the vicinity of 45°, we see that there is no great variation of the relative magnitudes of the cross sections of the
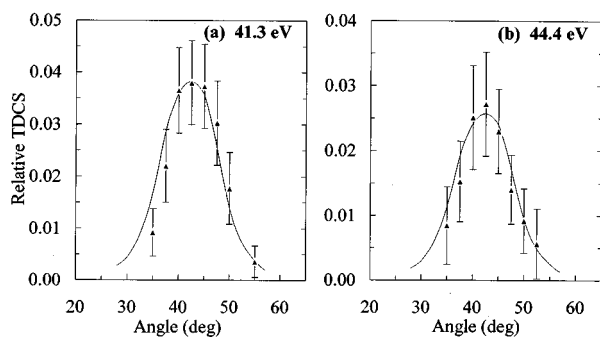
FIG. 4. 400 eV coplanar symmetric TDCS for ionization for the two satellite states of N_2^+ observed at 41.3 eV (a) and 44.4 eV (b) binding energy. — is the fitted curve to the experimental TDCS for the $2\sigma_g^{-1}$ ionic state [Fig. 2(d)]. Normalization as in Fig. 1.

different states when the energy decreases; however, there exist some modifications in shape which make a precise evaluation problematic.

C. Satellite structures

The differences observed between the TDCS of the ion states produced by single electron transitions help us to understand the type of correlations responsible for the satellite structures whose angular behaviors are shown in Fig. 4. The TDCS of the states located at 41.3 and 44.4 eV are weaker than those due to one electron transitions and present, as for the $(3\sigma_g)^{-1}$ and $(2\sigma_g)^{-1}$ ionic states, a maximum near 45°. Since their angular widths are the same as that observed for the $(2\sigma_g)^{-1}$ state, these structures, close in energy to the main peak at 38 eV, seem to be associated with ionization of the inner $2\sigma_g$ orbital. This is in agreement with the previous work of Weigold et al. [20] and Cook et al. [28], who demonstrated that ionization of this orbital leads not only to the broad structure at 38 eV but also to weaker structures located from 27 to 60 eV binding energy (which were partially resolved only in the later work). If the satellite structures are due to rearrangement in the residual ion, impulsive $(e,2e)$ and high energy PES spectra should be similar. However, comparisons of these spectra for Ar [34] and Xe [35] targets have shown up discrepancies in the relative intensities of the satellite states, due partly to the fact that the two types of spectroscopy probe different momentum regions of the electronic wave function. Amusia and Kheifets [27] have also pointed out the important role played by initial and final state correlation effects which can cause the relative intensities of the PES satellite states to deviate from the standard spectroscopic factors. In the PES work of Svensson et al. [36] and of Gelius et al. [37], made at 1487 eV on N_2, a broad main peak near 38 eV, dominated by ionization of the $2\sigma_g$ orbital, is found. On the high binding energy side of this, there is a clearly defined structure at 40.8 eV. Svensson et al. [36] also observe a structure near to 44 eV, superimposed on a strong continuum which makes precise determination of its intensity difficult. Both these structures are present in our $(e,2e)$ spectra and the intensity of that at 40.8 eV relative to the main peak seems in fact to be similar to that observed in PES. In the $(e,2e)$ experiments of Hamnett, Stoll, and Brion [38] which simulate PES, these structures are not resolved and appear as a shoulder on the 40 eV side of the main peak.
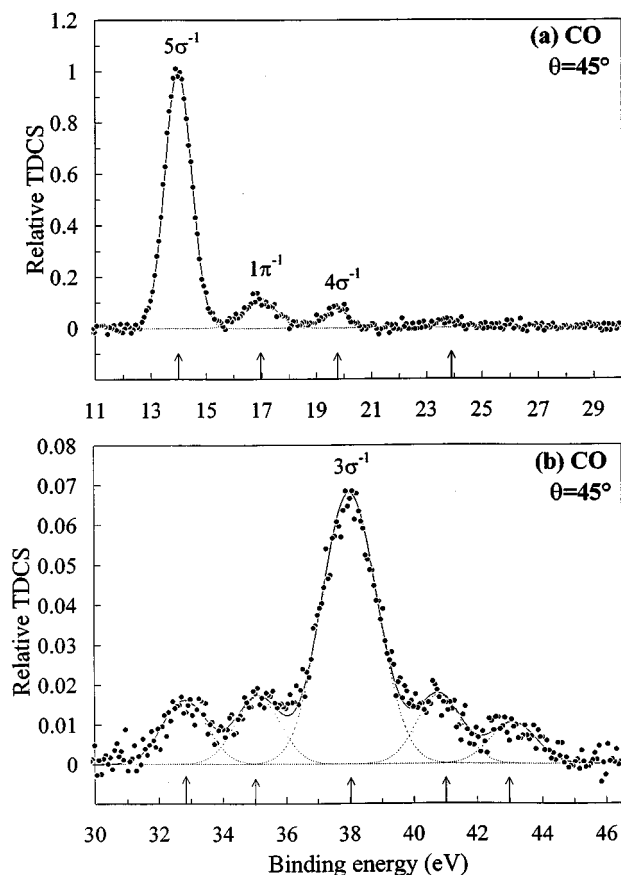

FIG. 5. Binding energy spectra of CO at 400 eV incident energy. In (a), the three first peaks correspond to the ionization of an electron from a particular molecular orbital. In (b), the broad peak is dominated by ionization from the 3σ orbital. The arrows indicate the positions of the observed ion states. Normalization as in Fig. 1.

V. THE CO MOLECULE

A. Binding energy spectra

The 11–30 eV binding energy spectrum of Fig. 5(a) was obtained at incident energy corresponding to $E_0=400$ eV, $\theta=45°$, and with an overall energy resolution of 1.2 eV. The three first peaks are due to the removal of an electron from the 5σ, 1π, and 4σ orbitals. They were less well resolved in the work of Dey et al. [21] but the relative intensities deduced from their spectrum taken at 400 eV, $\theta=42.3°$, and $\phi=0°$ are in good agreement with our measurements. We also observe a weaker structure at about 24 eV binding energy, not seen by them. Figure 5(b) shows our 30–46 eV binding energy spectrum obtained at $E_0=400$ eV incident energy and $\theta=45°$. This spectrum is clearly more complex than that for ionization of N_2 in the same binding energy region. The main peak at 38 eV corresponding to ionization of the 3σ orbital is, as in PES experiments [36,37], narrower than for N_2: its width is found to be about 2 eV. We observe additional weaker structures at approximately 32.8, 35, 41, and 43 eV. In contrast to the case of N_2, for CO, to the best of our knowledge, there exist no previous $(e,2e)$ measurements with a resolution comparable to our present one. We are able to obtain information on the structures comparable to that obtained by Cook et al. [28] for N_2.

B. Angular distributions

Our TDCS taken at $E_0=400$ eV and in a small angular region near 45° for ionization from the 5σ and 3σ orbitals, presented in Figs. 6(a) and 6(d), both have maxima near 45°. Nevertheless, as for N$_2$, the widths of these are found to be different. The cross sections for ionization from the two asymmetric orbitals in Figs. 6(b) and 6(c) have two peaks: the first, at low angles, is bigger than the second, at large angles. As above, we compare our measurements with PWIA calculations made using Snyder and Basch wave functions with relative normalization made as before. For the $(1\pi)^{-1}$, $(4\sigma)^{-1}$, and $(3\sigma)^{-1}$ ion states, disagreements between measurements and calculations are again observed at small angles.

To compare ionization dynamics for the two isoelectronic molecules N$_2$ and CO, measurements have been performed on CO over a large angular region at incident energies of $E_0=360$, 180, and 90 eV which bear the same relation to the ionization potential as the energies 400, 200, and 100 eV for N$_2$. At 360 eV, due to the small value of the cross section at large angle, we have only repeated measurements for the 5σ outermost orbital. As shown in Fig. 7 the TDCS of the different states of CO$^+$ have behavior identical in shape to that of the corresponding N$_2$ data in Fig. 3. To within experimental errors, identical relative intensity is also found for the $(1\pi)^{-1}$ and $(4\sigma)^{-1}$ ionic states. The only difference between the ionization of the two molecules concerns ionization of the inner 3σ orbital of CO [Fig. 7(d)], for which the TDCS are of smaller relative intensity by a factor of around 1.5 than that for ionization of the $2\sigma_g$ orbital of N$_2$. On the energy range under study, the absence of a center of symmetry at the midpoint of the distance of the two nuclei in the CO molecule seems to have an insignificant effect on the angular distribution of the TDCS, except for the innermost orbital. The construction of molecular orbitals by the linear combination of atomic orbitals (LCAO) method is in fact almost identical for CO and for N$_2$. The $2\sigma_g$ (3σ) and $2\sigma_u$ (4σ)
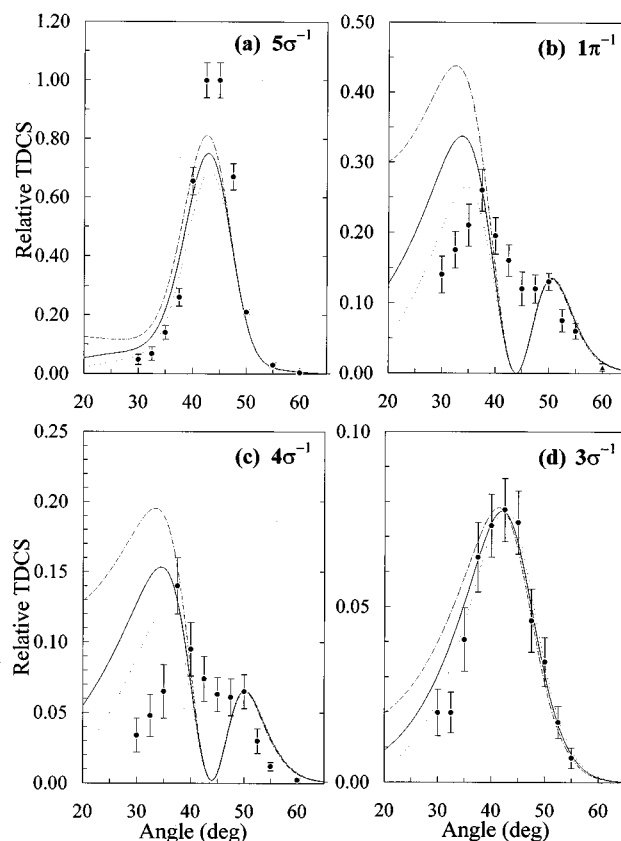

FIG. 6. 400 eV coplanar symmetric TDCS for ionization from the 5σ (a), 1π (b), 4σ (c), and 3σ (d) orbitals of CO. PWIA calculations for the Ford (—), regularized (---), and standard ($\cdots$) forms of the half-off-shell Coulomb T matrix. Theoretical calculations are normalized to the data for ionization from the 4σ orbital at 50° except in (d) where they are normalized to the data at 42.5°.
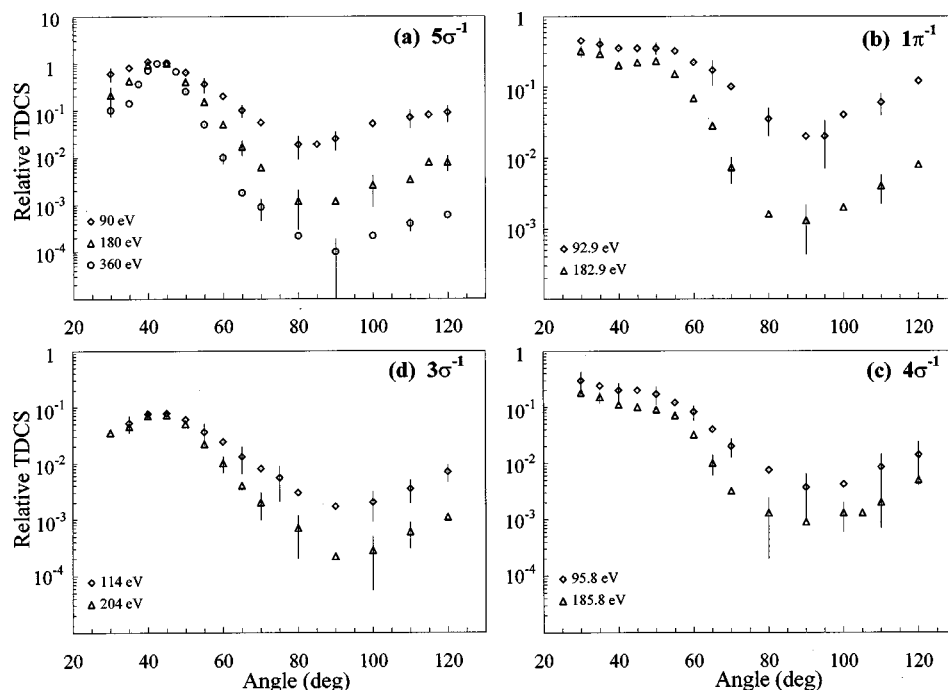

FIG. 7. Coplanar symmetric TDCS for ionization from the 5σ (a), 1π (b), 4σ (c), and 3σ (d) orbitals of CO. The energy E_0 is 90 eV ($\diamond$), 180 eV ($\triangle$), and 360 eV ($\bigcirc$). Normalization as in Fig. 1.
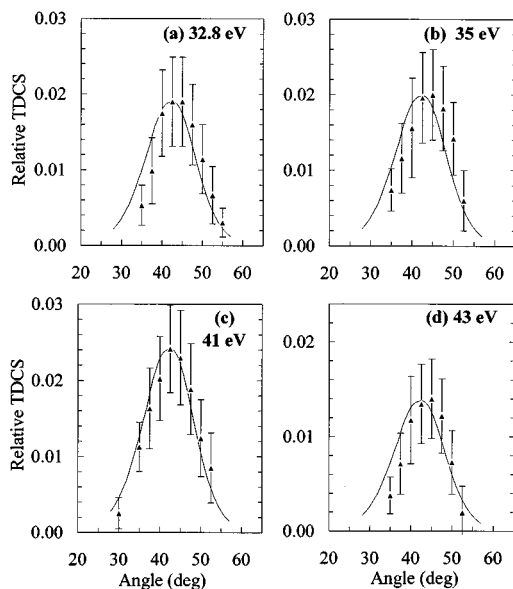
FIG. 8. 400 eV coplanar symmetric TDCS for the satellite states of CO^+ observed at 32.8 eV (a), 35 eV (b), 41 eV (c), and 43 eV (d) binding energy. — is the fitted curve to the experimental TDCS for the $3\sigma^{-1}$ ion state [Fig. 6(d)]. Normalization as in Fig. 1.
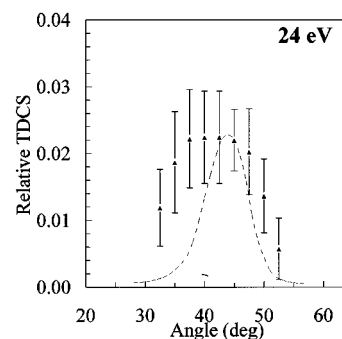

FIG. 9. 400 eV coplanar symmetric TDCS for the satellite state of CO^+ observed at about 24 eV binding energy. --- is the fitted curve to the experimental TDCS for the $5\sigma^{-1}$ ionic state [Fig. 6(a)]. Normalization as in Fig. 1.

orbitals come mainly from even and odd overlaps, respectively, of atomic 2*s* orbitals centered on the respective nuclei. The $3\sigma_g$ (5σ) orbital comes mainly from an even overlap of atomic 2*p* orbitals aligned along the molecular axis whereas the $1\pi_u$ (1π) orbital comes from an odd overlap of 2*p* orbitals aligned perpendicularly to it [39]. Furthermore, the interaction between the incident electron and the permanent dipole momentum of CO apparently induces no modifications of the TDCS. Similar behavior in both molecules of the elastic scattering cross sections, in the same energy region and over similar angular range, was found by Bromberg [40] and by Dubois and Rudd [41]. The absence of differences is due either to the weakness of this interaction or to the effect of the random orientation of the molecules in the gas beam.

C. Satellite structures

In Fig. 8, the angular behavior of the TDCS is shown for the structures which appear in the binding energy spectrum on both sides of the main peak. The distributions have a single maximum near 45° and so must be explained principally by the effect of correlations between valence excited states and σ^{-1} type ion hole states. These could be either the $(5\sigma)^{-1}$ or the $(3\sigma)^{-1}$ state, but the experimental cross sections for all the satellite states have quite the same angular width as those for the $(3\sigma)^{-1}$ state. Thus the dominant process seems to be correlation involving the latter. The early experiments of Dey *et al.* [21], made principally at 1200 eV, do not resolve the structures due to correlations in the target. To analyze their data, they selected particular (theoretical) energy positions; they then compared the magnitudes of the cross section at these positions. Their results appeared to indicate a strong correlation with the $(3\sigma)^{-1}$ state in the range of 28–60 eV binding energy. But in view of the poor precision, they could not exclude the possibility of admixtures of the other σ^{-1} states which is expected on theoretical

grounds. They note that the observation in detail of the predicted configuration interaction effects requires superior count rate and resolution to theirs. The fact that we see no evidence of admixture in our high-resolution experiments is therefore of interest.

The high-resolution PES study of Svensson *et al.* [36] reveals numerous states between 30 and 38 eV binding energy, while Gelius *et al.* [37], using poorer-resolution PES, find broad structures near 32 and 35.7 eV. Above 38 eV they observe two small structures at 41 and 43 eV. The contribution of the continuum is extremely difficult to estimate in this energy region so determination of the relative intensity of the structures is necessarily imprecise. We observe structures in (*e*,2*e*) near 32.8 and 35 eV which, on the basis of the observations of Svensson *et al.* [36], correspond in fact to several different states overlapping. However, the resolution of our experiments is not yet sufficient to resolve these structures with the precision of recent PES measurements. The global intensities of these structures seem to be slightly larger in our spectrum. We also find structures near 41 and 43 eV, apparently with higher intensities than seen by Gelius *et al.* [37]. In the work of Svensson *et al.* [36] there is a further, quite large, satellite structure at 23.7 eV. It is also seen in the PES work of Gelius *et al.* [37] and Hamnett, Stoll, and Brion [38]. We observe a structure near 24 eV whose intensity is sufficient for us to be able to investigate the angular behavior of the TDCS, shown in Fig. 9. This is radically different from the behavior observed for the other satellites. This structure is located closer in energy to the $(5\sigma)^{-1}$, $(1\pi)^{-1}$, and $(4\sigma)^{-1}$ ionic states than to the $(3\sigma)^{-1}$ one. Correlation effects with the outermost ionic hole states are therefore to be expected to be important. The differences observed between the TDCS of the satellite structure and of the $(5\sigma)^{-1}$ ionic state could be induced by correlation effects with the $(1\pi)^{-1}$ or $(4\sigma)^{-1}$ states. Since correlations with the $(1\pi)^{-1}$ state are known to be very weak, it seems that the structure at 24 eV is associated with a shake-up process involving the 4σ orbital, as was pointed out in the analysis of the PES experiments [36].

VI. CONCLUSION

Cross sections for electron impact ionization of the N_2 and CO molecules between 90 and 400 eV incident energy in a coplanar symmetric energy sharing geometry have been

presented. To the best of our knowledge, these are the only TDCS for molecules available in this kinematical arrangement and for such an energy range. We have found that our TDCS at 400 eV in the low angle region are not well reproduced by calculations made using the plane wave impulse approximation, contrary to the findings of previous experiments made in noncoplanar symmetric and coplanar asymmetric geometries. Three prescriptions are used to evaluate the half-off-shell Coulomb T matrix which the PWIA requires. All of them overestimate the TDCS in the low angle region, inducing shifts of the primary (binary collision) maximum towards small angles. In addition, calculations for orbitals of π symmetry predict a cross section going to zero at about 45°, whereas the minimum which we observe is less pronounced. This difference cannot be explained by our finite angular resolution: the discrepancies between theory and experiment are real. Among probable causes, there are ACB and perhaps also PCI dynamical effects. A first step to correction of the PWIA is the replacement of plane waves by distorted waves, but this requires making a ''factorization'' approximation, the validity of which is difficult to justify other than by hand-waving arguments. Our experience with atomic targets, however, leads us to hope that this would resolve certain discrepancies and permit meaningful calculation in the region of the secondary (backscattering) maximum. But what is really needed is a DWBA type model including ACB and PCI effects explicitly. As the incident energy is decreased, the minimum at about 45° for electron detachment from π orbitals progressively disappears. This behavior is similar to that observed in the case of ionization of p orbitals of rare gas targets. For detachment both from σ and from π molecular orbitals, the relative intensity of the backward peak increases with decreasing energy. This effect, due to the onset of multiple collision phenomena, is strongest in the π case, presumably because the wave function is concentrated less into the region near axis, between the two nuclei. No effects, such as the appearance of new structures, attributable to the two-center nature of the projectile-nuclear forces or to the different nuclear structures of the N_2 and CO molecules have been observed in the present work. Perhaps they might be seen in similar experiments either at lower energies or on oriented target molecules; we plan in the near future to study the ionization mechanism down to threshold on another apparatus currently being installed. In addition, our high energy resolution allows us to observe separated peaks corresponding to residual ion final states differing in energy because of correlation effects. The analysis of the weakly excited states located from 32 to 45 eV binding energy confirms their strong correlation with inner hole states of the molecules.

[1] H. Ehrhardt, K. Jung, G. Knoth, and P. Schlemmer, Z. Phys. D **1**, 3 (1986).

[2] I. E. McCarthy and E. Weigold, Rep. Prog. Phys. **51**, 299 (1988).

[3] M. A. Coplan, J. H. Moore, and J. P. Doering, Rev. Mod. Phys. **66**, 985 (1994).

[4] A. Pochat, R. J. Tweed, J. Peresse, C. J. Joachain, B. Piraux, and F. W. Byron, J. Phys. B **16**, L775 (1983).

[5] L. Frost, P. Freienstein, and M. Wagner, J. Phys. B **23**, L715 (1990).

[6] T. Rösel, C. Dupré, J. Röder, A. Duguet, K. Jung, A. Lahmam-Bennani, and H. Ehrhardt, J. Phys. B **24**, 3059 (1991).

[7] T. Rösel, J. Röder, L. Frost, K. Jung, H. Ehrhardt, S. Jones, and D. H. Madison, Phys. Rev. A **46**, 2539 (1992).

[8] J. Röder, K. Jung, and H. Ehrhardt, J. Phys. (France) IV **3**, C6-29 (1993).

[9] S. Rioual, A. Pochat, F. Gélébart, R. J. Allan, C. T. Whelan, and H. R. J. Walters, J. Phys. B **28**, 5317 (1995).

[10] J. Rösel, K. Jung, H. Ehrhardt, X. Zhang, C. T. Whelan, and H. R. J. Walters, J. Phys. B **23**, L649 (1990).

[11] S. Bell, C. T. Gibson, and B. Lohmann, Phys. Rev. A **51**, 10 252 (1995).

[12] C. T. Whelan, H. R. J. Walters, R. J. Allan, and X. Zhang, in (*e,2e*) *and Related Processes*, edited by C. T. Whelan, H. R. J. Walters, A. Lahman-Bennani, and H. Ehrhardt (Kluwer, Dordrecht, 1993), pp. 1–32.

[13] C. T. Whelan, R. J. Allan, J. Rasch, H. R. J. Walters, X. Zhang, J. Röder, K. Jung, and H. Ehrhardt, Phys. Rev. A **50**, 4394 (1994).

[14] M. Nicolas, R. J. Tweed, and O. Robaux, J. Phys. B **29**, 791 (1996).

[15] F. Rouet, R. J. Tweed, and J. Langlois, J. Phys. B **29**, 1767 (1996).

[16] K. Jung, E. Schubert, D. A. L. Paul, and H. Ehrhardt, J. Phys. B **8**, 1330 (1975).

[17] L. Avaldi, R. Camilloni, E. Fainelli, and G. Stefani, J. Phys. B **25**, 3551 (1992).

[18] L. Avaldi, R. Camilloni, and G. Stefani, Phys. Rev. A **41**, 134 (1990).

[19] M. Cherid, A. Lahmam-Bennani, A. Duguet, R. W. Zurales, R. R. Lucchese, M. C. Dal Cappello, and C. Dal Cappello, J. Phys. B **22**, 3483 (1989).

[20] E. Weigold, S. Dey, A. J. Dixon, I. E. McCarthy, K. R. Lassey, and P. J. O. Teubner, J. Electron Spectrosc. Relat. Phenom. **10**, 177 (1977).

[21] S. Dey, A. J. Dixon, K. R. Lassey, I. E. McCarthy, P. J. D. Teubner, E. Weigold, P. S. Bagus, and E. K. Viinikka, Phys. Rev. A **15**, 102 (1977).

[22] L. Avaldi, R. Camilloni, E. Fainelli, and G. Stefani, J. Phys. B **20**, 4163 (1987).

[23] I. E. McCarthy and M. J. Roberts, J. Phys. B **20**, L231 (1987).

[24] J. C. Y. Chen and A. C. Chen, Adv. At. Mol. Phys. **8**, 71 (1972).

[25] W. F. Ford, Phys. Rev. **133**, B1616 (1964).

[26] M. J. Roberts, J. Phys. B **18**, L707 (1985).

[27] M. Y. Amusia and A. S. Kheifets, J. Phys. B **18**, L679 (1985).

[28] J. P. D. Cook, R. Pascual, E. Weigold, W. Von Niessen, and P. Tomasello, Chem. Phys. **141**, 211 (1990).

[29] M. Vos, S. A. Canney, P. Storer, I. E. McCarthy, and E. Weigold, Surf. Sci. **327**, 387 (1995).

[30] A. Pochat, X. Zhang, C. T. Whelan, H. R. J. Walters, R. J. Tweed, F. Gélébart, M. Cherid, and R. J. Allan, Phys. Rev. A **47**, R3483 (1993).

[31] L. C. Snyder and H. Basch, *Molecular Wave Functions and Properties* (Wiley, New York, 1972).

[32] I. Fuss, I. E. McCarthy, C. J. Noble, and E. Weigold, Phys. Rev. A **17**, 604 (1978).

[33] P. Duffy, M. E. Casida, C. E. Brion, and D. P. Chong, Chem. Phys. **159**, 347 (1992).

[34] I. E. McCarthy, R. Pascual, P. Storer, and E. Weigold, Phys. Rev. A **40**, 3041 (1989).

[35] S. Braidwood, M. Brunger, and E. Weigold, Phys. Rev. A **47**, 2927 (1993).

[36] S. Svensson, M. Carlsson-Göthe, L. Karlsson, A. Nilson, N. Martensson, and U. Gelius, Phys. Scr. **44**, 184 (1991).

[37] U. Gelius, E. Basilier, S. Svensson, T. Bergmark, and K. Siegbahn, J. Electron Spectrosc. Relat. Phenom. **2**, 405 (1974).

[38] A. Hamnett, W. Stoll, and C. E. Brion, J. Electron Spectrosc. Relat. Phenom. **8**, 367 (1976).

[39] J. C. Slater, *Quantum Theory of Molecules and Solids: Electronic Structure of Molecules* (McGraw-Hill, New York, 1963), Chap. 6.

[40] J. P. Bromberg, J. Chem. Phys. **50**, 3906 (1969); **52**, 1243 (1970).

[41] R. D. DuBois and M. E. Rudd, J. Phys. B **9**, 2657 (1976).